



## RESEARCH ARTICLE OPEN ACCESS

# Electrospun Poly (Glycerol Sebacate) (PGS) Membranes for Corneal Tissue Engineering

 Sumeyye Narin<sup>1</sup>  | Sevilay Burcu Sahin<sup>1</sup> | Ebru Demir<sup>1</sup> | Sibel Cetinel<sup>1,2</sup> 
<sup>1</sup>Sabanci University Materials Science and Nano Engineering Department, Molecular Biology, Genetics, and Bioengineering Department, Sabanci University, Istanbul, Turkiye | <sup>2</sup>Sabanci University Nanotechnology Research and Application Center (SUNUM), Istanbul, Turkiye

**Correspondence:** Sibel Cetinel ([cetinel@sabanciuniv.edu](mailto:cetinel@sabanciuniv.edu))

**Received:** 15 April 2025 | **Revised:** 28 May 2025 | **Accepted:** 16 June 2025

**Funding:** This work was funded by 2232 International Fellowship for Outstanding Researchers Program of TUBITAK (Grant number 118C371).

**Keywords:** human corneal endothelial cells | human corneal epithelial cells | poly glycerol sebacate (PGS) | regeneration

## ABSTRACT

The demand for corneal tissue replacements increases due to corneal diseases, prompting the exploration of tissue engineering (TE) solutions using biopolymers. Poly (glycerol sebacate) (PGS) is one of the promising biomaterials to be explored in the ocular TE, not only because of its biocompatibility, biodegradability, and elasticity, but also its transparency. However, its low molecular weight and low glass transition temperature ( $T_g$ ) make PGS scaffold fabrication via electrospinning challenging. Here, we fabricated fibrous membranes by electrospinning of PGS and poly (vinyl alcohol) (PVA) blend and obtained a membrane composed of homogenous fibers with a diameter of 4  $\mu\text{m}$  and a porosity of 28%. In addition, the membrane exhibited a stiffness of 12 MPa and strain of 20%. The permeability of the membrane closely resembled that of the natural cornea with  $9.8\text{E-}07\text{ cm}^2/\text{s}$ . Most of the PVA was successfully washed off, resulting in biocompatible scaffold that was able to support the proliferation of human corneal epithelial cells (HCEC) and human corneal endothelial cells (HCEndC) for a week. According to the in vitro biocompatibility assay, HCEC has demonstrated an 88% and HCEndC a 96% viability on electrospun PGS membranes. These results demonstrate the suitability of electrospun PGS membrane for cornea tissue engineering.

## 1 | Introduction

The human cornea is a transparent, and avascular tissue providing a barrier, and a protective layer for the eye against both mechanical damage and infections [1]. It consists of three distinct cellular layers within 0.5 mm thickness [2]: corneal epithelium, stroma and endothelium that are connected by acellular junctions, Bowman's layer and Descemet's membranes [3]. The epithelium is located in the outer layer of the cornea and is responsible for the regulation of water and soluble components transfer, and functions as the biological barrier [4]. Due to its direct exposure to the external environment, the epithelial layer is more prime to injuries such as corneal abrasion, erosion, ulcer, and dystrophies, mostly leading to blurriness in vision or even vision loss [5, 6]. Treatment of such diseases with pene-

trating keratoplasty, anterior lamellar keratoplasty (ALK) or deep anterior lamellar keratoplasty (DALK) results in over 180 000 corneal transplant operations per year, globally [7]. Despite the efficient outcomes of keratoplasty operations, the shortage of donor corneas necessitates the investigation of alternative solutions focusing on tissue engineering applications to generate transplantable engineered tissues [8].

The initial design parameter for corneal epithelial tissue engineering is to find the ideal biomaterial, which should possess good biocompatibility, and transparency. Collagen, as being one of the natural components of the cornea, is the most widely used biomaterial for generation of corneal tissue substitutes, providing optical clarity, mechanical strength, and elasticity both in vitro and in vivo [9, 10]. However, collagen-based

This is an open access article under the terms of the [Creative Commons Attribution](https://creativecommons.org/licenses/by/4.0/) License, which permits use, distribution and reproduction in any medium, provided the original work is properly cited.

© 2025 The Author(s). *Macromolecular Materials and Engineering* published by Wiley-VCH GmbH

scaffolds require complicated chemical cross-linking steps and are not cost effective [11]. Alternatively, synthetic polymers such as poly(methyl-methacrylate) (PMMA), poly (lactic-co-glycolic acid) (PLGA), and polycaprolactone (PCL) are investigated [12]. The most promising synthetic polymer to date is poly (N-isopropylacrylamide) (PNIPAAm) that has already been applied clinically with corneal epithelial cells, however, requires irradiation or temperature for the cross-linking [13].

Recently, a tough elastomer called PGS that provides transparency, biocompatibility and composed of monomers approved by the Food and Drug Administration (FDA) stands out [14]. This material is relatively inexpensive as a result of its monomers' origin [14] and exhibits properties of thermoset elastomers [15]. Furthermore, PGS's degradation products, glycerol and sebacic acid, naturally exist in the body [14, 16]. Additionally, the material can be designed to obtain higher mechanical properties and to target different degradation rates based on application [17]. PGS can be utilized for engineering of a variety of tissues including soft tissues [16], such as adipose [18], cartilage [15], cardiac [19, 20], vascular [21], tendon [22], retinal [23, 24], and corneal [25–28] tissues. Salehi et al. proved that the viability of human corneal epithelial cells on PGS films was comparable to that of the control group, with a 90% viability rate [14, 25]. However, it is important for corneal tissues to be permeable for water uptake. To achieve the required permeability, a porous scaffold can be fabricated by using electrospinning [29]. Even so, electrospinning of PGS is difficult due to its low molecular weight and a melting temperature that's lower than its cross-linking temperature [29, 30]. To overcome these obstacles, PGS has been blended with a variety of high molecular weight carrier polymers including poly (caprolactone) PCL [31], poly (lactic acid) (PLLA) [18, 32], and poly (vinyl alcohol) (PVA) [33].

The immunocompatibility of PGS-PCL nanofibrous scaffolds has been demonstrated for HCECs [27] and human corneal conjunctival endothelial cells [11, 26]. Similarly, fibrous membranes obtained from PVA-PGS blends have been shown to be biocompatible for mouse fibroblast cells [34]. Yet, the carrier polymer ought to be removed from the membranes if it is expected to show pure PGS properties. Because of its high water solubility, PVA is an efficient candidate, which can be removed from the system by simply dissolving in water.

Here, we used PVA as the carrier for the fabrication of porous PGS membranes by electrospinning to mimic the native tissue microenvironment of the corneal epithelial and endothelial layers. The PVA was chosen due to its water solubility, allowing for easy removal by water wash after PGS cross-linking [29]. The resulting membranes were characterized for their chemical structure, transparency, mechanical strength, and permeability, and their *in vitro* biocompatibility was evaluated with HCECs and HCEndCs.

## 2 | Results and Discussion

### 2.1 | prePGS Synthesis and Electrospinning

The PGS prepolymer (prePGS) was synthesized by the esterification of glycerol and sebacic acid through a reversible reaction of

the primary hydroxyl groups in glycerol with carboxyl groups in sebacic acid, resulting in a polyester and water as a by-product (Figure 1) [14]. The molecular weight of the obtained prepolymer was around 50.000 g/mol according to GPC analysis (Figure S1). The FT-IR spectrum of PGS exhibits generally similar peaks with PVA that causes peak differentiation to be harder as can be seen in Figure S2. The peak observed between 3500 and 3000  $\text{cm}^{-1}$  due to -OH stretching exists in both polymers [29]. However, the PGS can be distinguished by a slight change in this peak where the OH stretching is mainly focused at 3450  $\text{cm}^{-1}$  for PGS and at 3300  $\text{cm}^{-1}$  as a broader peak for PVA. Another similarity can be observed at around 2900 and 2800  $\text{cm}^{-1}$  corresponding to alkane stretching that exists in both polymers, yet, for the PGS, this peak is mainly focused at 2900  $\text{cm}^{-1}$  with a small peak on the left where it is clearly two-shouldered. The only characteristic peaks for PGS resided at 1740 and 1200  $\text{cm}^{-1}$  for  $\text{C}=\text{O}$ , and  $\text{C}-\text{O}$  stretching due to the carboxylic acid group of sebacic acid in PGS [29, 35]. The characteristic small peak at 840  $\text{cm}^{-1}$  is specific to PVA and observed in the cross-linked membranes as well (Figure 2A; Figure S2) [33].

The corneal layers are composed of uniformly distributed collagen fibrils, and its high-oriented structure reduces forward light scattering and enhances the mechanical strength and transparency [36]. To achieve a fibrous scaffold, prePGS was electrospun resulting in uniform fibrils resembling the collagens. The optimum electrospinning solution was obtained by using a 5.8 wt.% 55:45 prePGS: PVA (molar ratio) blend dissolved in hexafluoro isopropanol (HFIP) overnight. The average fiber diameter was 4.21  $\mu\text{m}$ . At this fiber diameter, electrospun membranes were transparent enough to allow reading through (Figure 2C).

### 2.2 | Cross-Linking and PVA Removal

PGS exhibits a low  $T_g$ , making it a viscous fluid that cannot retain its shape. Therefore, following the shaping of prePGS into a membrane, it requires a secondary cross-linking. Also, it is known that thermoset polymers such as PGS exhibit different optical and mechanical properties according to cross-linking density. As the cross-linking temperature increases, the cross-linking degree of PGS also increases [37]. Accordingly, after obtaining the intact electrospun PGS membranes, the effect of cross-linking temperature was investigated considering two factors: cross-linking density and fiber stability (after cross-linking and PVA removal). For this purpose, PGS membranes were crosslinked at different temperatures ranging from 140°C to 170°C for 48 h. The FT-IR analysis exhibited a broad peak around 3300  $\text{cm}^{-1}$  corresponding to the secondary -OH groups' stretching of both polymers, PGS and PVA [38]. Since this group is utilized for cross-linking, when the cross-linking degree is increased, a reduction in the OH peak is expected. In Figure 2A, the OH peak reduction can be observed as the temperature increases from 140°C to 160°C indicating 160°C cross-linking temperature provided the highest cross-linking. However, when the temperature of cross-linking is set to 170°C, there is no reduction in the peak that might be due to the increased mobility of PVA chains at elevated temperatures, which may interfere with further cross-linking of PGS. At 170°C, the enhanced mobility of PVA could disrupt the polymer network, limiting effective esterification and preventing additional OH

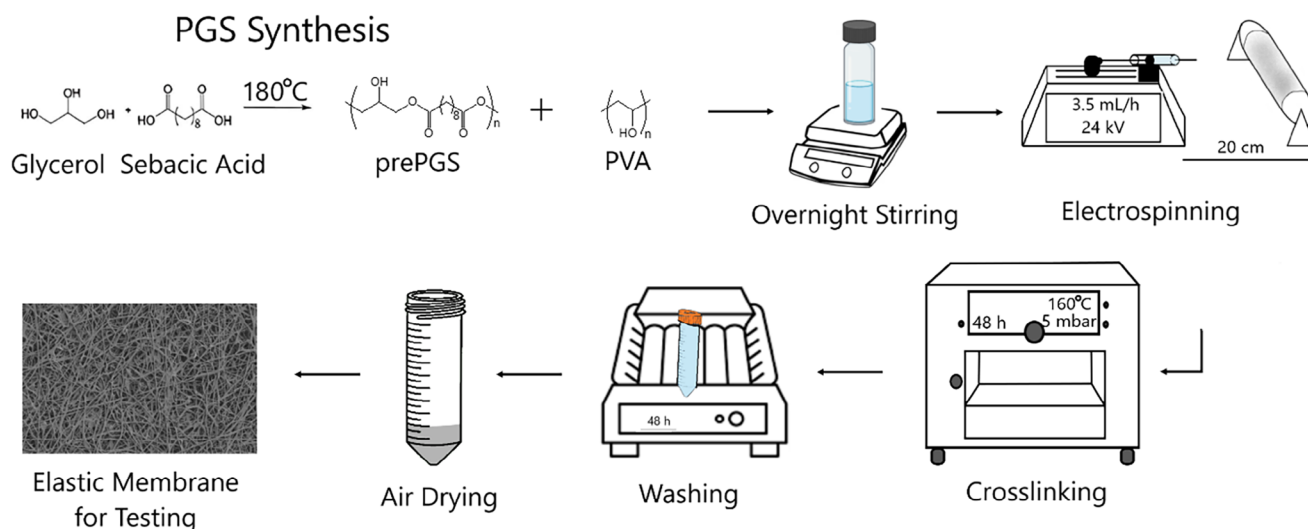


**FIGURE 1** | Schematic representation for the fabrication of fibrous PGS-PVA sheets as corneal membranes. In the first stage of preparation, prePGS was synthesized and blended with PVA by overnight stirring, and the resulting solution was electrospun. At the second stage, the obtained membrane was cross-linked in a vacuum oven to preserve its fibrous shape, and PVA was removed by washing with water and air drying.

consumption. Moreover, minor thermal degradation of PVA at this temperature may expose free hydroxyl groups, contributing to the stabilization of the OH peak. These findings align with previous studies on PVA's thermal behavior, where increased temperature led to chain rearrangement and hindered further cross-linking [39].

It is reported that PVA-PGS membranes did not cover all properties of the pure PGS and need to be removed from the system following a series of washings [14, 29]. The removal of PVA after cross-linking of PGS membrane is important to obtain pure PGS and thereby increase elasticity and transparency of the membranes, which are important parameters for mimicking corneal tissue. As PVA can be dissolved in water -without the necessity of possibly toxic organic solvents—a variety of washing methods can be applied [40]. Accordingly, water wash at room temperature and 60°C as well as 70% ethanol were evaluated for the membranes produced at 160°C cross-linking temperature. The 24 h water wash followed with an hour ethanol wash to remove PVA and residual PGS monomers resulted in diminishment of peaks at 3300 and 840  $\text{cm}^{-1}$  corresponding to —OH stretching and —C—O stretching of PVA, respectively (Figure 2B) [33]. Further PVA removal was observed by extending the duration of water wash up to 48 h. Other peaks including —C=O stretching of the carboxylic acid group of sebacic acid in PGS at 1740  $\text{cm}^{-1}$  was preserved after washings (Figure 2A) [29, 35]. The peaks at the range of 1100 and 900  $\text{cm}^{-1}$  in the characteristic region corresponds to —C—O stretching due to primary and secondary -OH groups in both PGS and PVA [18, 29, 33].

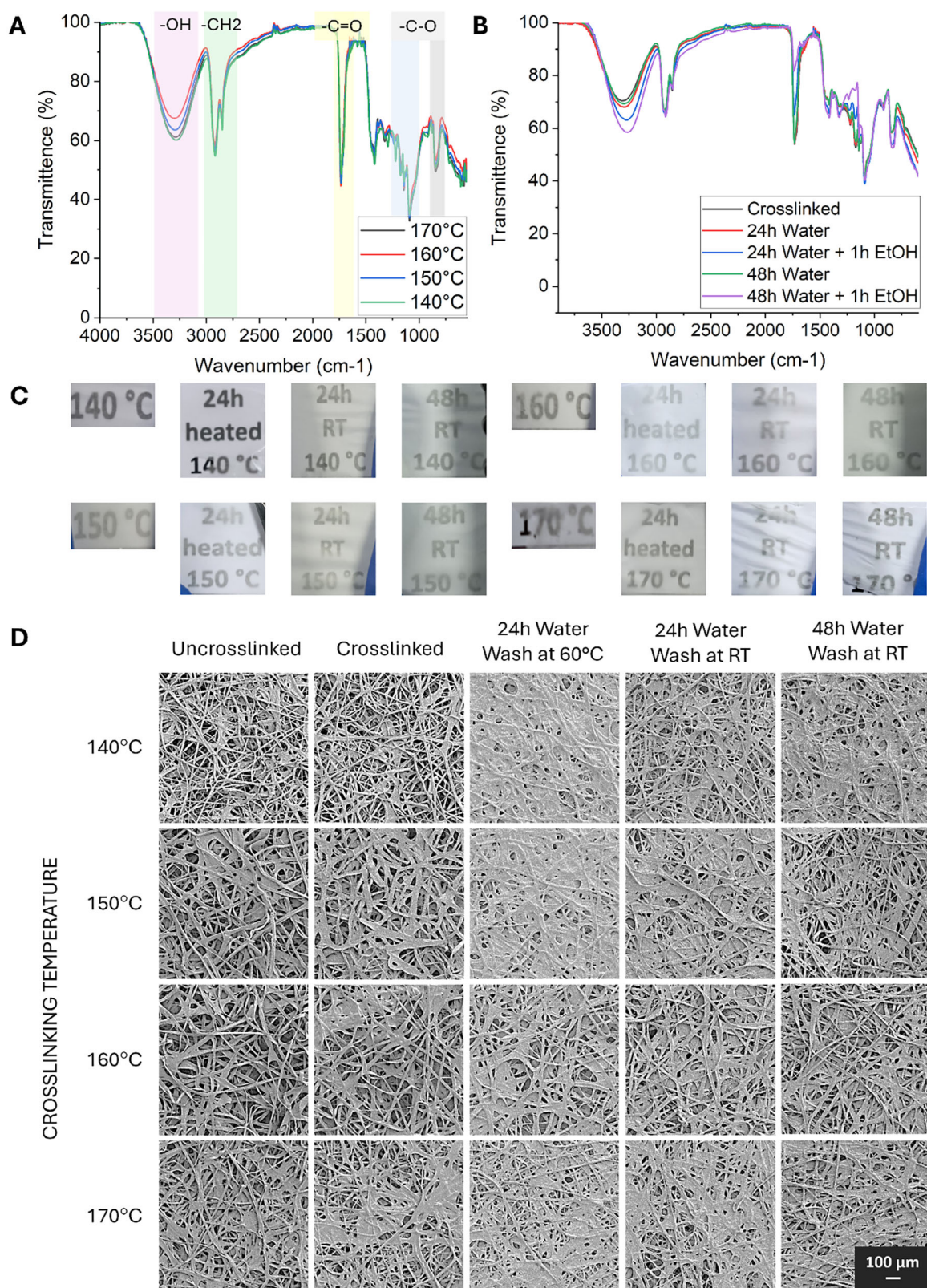
When the fibers fuse into sheets, membranes become more transparent due to reduced reflection of light in a less porous environment. Therefore, 140°C, 150°C, and 170°C cross-linking temperatures generated more transparent membranes (Figure 2C). Accordingly, the membranes crosslinked at 160°C were less transparent compared to others; despite the fact that they were transparent enough to read the writings under the membrane.

SEM visualization indicated that the cross-linking temperatures of 140°C, 150°C, and 160°C resulted in good fiber stability after cross-linking (Figure 2D). However, membranes crosslinked at 170°C were fused into a sheet (Figure 2D). On the other hand, the membranes crosslinked at 140°C, 150°C, and 170°C were not durable enough to support the fibrous structure during water/ethanol wash, as fibers collapsed, yielding a less porous structure. The optimal cross-linking temperature that could withstand washings to remove the PVA, retain fiber morphology, and ensure good porosity, was found to be 160°C. Since the crosslinking temperature of 160°C provided the best fiber stability and its transparency was sufficient, further characterizations were made with this membrane (Table 1).

The instability of membranes crosslinked at 140°C and 150°C can be attributed to insufficient cross-linking, resulting in a weaker polymer network that fails to maintain fiber integrity during washing. At these temperatures, the cross-linking density is inadequate to provide the necessary mechanical stability, leading to fiber collapse upon exposure to solvents. This observation aligns with findings from studies on PGS-based electrospun fibers, where lower cross-linking temperatures (24 h at 120°C followed by 48 h at 140°C) resulted in reduced structural integrity [41]. Conversely, membranes crosslinked at 170°C exhibit instability due to excessive polymer chain mobility of PVA, causing fibers to fuse into a sheet-like structure [39]. This fusion diminishes porosity and compromises the membrane's ability to withstand washing, as the interconnected fibrous architecture is lost. Similar phenomena have been reported in studies where higher cross-linking temperatures (24 h at 120°C followed by 48 h at 140°C and 24 h at 170°C) led to fiber merging and loss of structural integrity of PGS-based electrospun fibers [41].

In contrast, cross-linking at 160°C provides an optimal balance, ensuring sufficient cross-linking to maintain fiber stability while preventing excessive fusion. This condition allows the membrane to retain its fibrous morphology and porosity, making it the most suitable for further characterization. This optimal

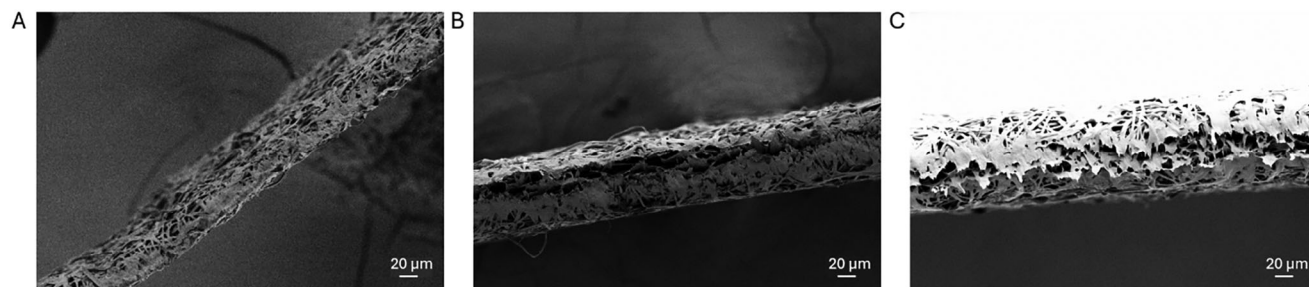




**FIGURE 2** | Characterization of membranes by FT-IR according to cross-linking temperatures (black, red, blue and green lines represent cross-linking temperatures of 170°C, 160°C, 150°C, and 140°C, respectively) (A) and removal of PVA from the membranes (black line: crosslinked membrane, red line: crosslinked membrane washed in water 24 h, blue line: crosslinked membrane washed in water 24 h and then in ethanol for 1 h, green line: crosslinked membrane washed in water 48 h, and purple line: crosslinked membrane washed in water 24 h and then in ethanol for 1 h) (B). The photographs of transparent membranes on written text (C) and their SEM images (D).

**TABLE 1** | Property outcomes of the different cross-linking temperatures.

Cross-linking temperature	Fiber stability after cross-linking	Fiber stability after wash steps	Transparency	PVA elimination
140°C	+	–	+	–
150°C	+	–	+	+
160°C	+	+	+	+
170°C	–	–	+	–

**FIGURE 3** | The cross-sectional SEM images of PGS membranes produced with 8 mL (A), 16 mL (B), and 24 mL (C) spin solutions resulting in -29  $\mu\text{m}$  (A), -59  $\mu\text{m}$  (B), and -82  $\mu\text{m}$  (C) average thickness. The average thickness values are obtained from 4 measurements for each sample.

temperature aligns with findings in similar studies, where controlled cross-linking conditions preserved fiber structure and functionality.

### 2.3 | Membrane Thickness

The normal cornea thickness would reach to 536  $\mu\text{m}$  on average [42, 43] whereas Bowman layer to 15  $\mu\text{m}$  thickness, and Descemet's membrane to 10  $\mu\text{m}$  thickness [4]. It is significant to achieve appropriate stiffness in tissue engineered scaffolds to obtain proper barrier function of cornea, defending the eye from mechanical damages and infections [1]. Therefore, besides the cross-linking parameters, the thickness of the membranes was also evaluated with an aim to obtain mechanically durable and persevered transparency. For this purpose, different amounts of spin solutions (8, 16, and 24 mL) were used to electrospun membranes in varying thicknesses. The membranes obtained with 8 mL of spin solution were extremely sensitive to external force, even held in hand. Hence, it was a necessity to increase the thickness of the membrane to increase strength and elasticity despite the fact that the natural corneal layers are thinner. The membrane that was spun with 8 mL of spin solution had 30  $\mu\text{m}$  thickness, and this value was doubled to 60  $\mu\text{m}$  with 16 mL, and was further increased to 82  $\mu\text{m}$  with 24 mL spins (Figure 3).

Membranes produced at varying thicknesses (29, -59, and -82  $\mu\text{m}$ ) were further analyzed for fiber structure and transparency while keeping the cross-linking parameters, 160°C for 48 h, constant. According to SEM images, the fiber morphology was not significantly affected by the change in the spinning solution amount (Figure 4A). Also, the cross-linking and the water washes did not alter the fiber shape and diameters (Figure 6B), indicating that between 29 and 82  $\mu\text{m}$  thicknesses, cross-linking at 160°C for

48 h is sufficient. In a similar study, the removal of PVA resulted in the disappearance of a snowflake-like morphology, confirming the successful elimination of the PVA shell and leaving behind PGS-rich porous fiber mats. Interestingly, a thin polymer film containing pores was observed around the remaining PGS fibers, which was attributed to either fiber adhesion or a transesterification reaction between PVA and the PGS prepolymer during curing [34]. While such a reaction was reported at 130°C, the membranes in this study were crosslinked at 160°C, a temperature at which secondary reactions are less likely to occur, preserving the fibrous structure.

When the fibers fuse into sheets, membranes become more transparent due to reduced reflection of light in a less porous environment [44]. Therefore, the transparency of the membranes with higher thickness is expected to decrease accordingly, due to the increase in the porosity of the membrane. Accordingly, the transparency of the 30  $\mu\text{m}$  crosslinked membrane was the highest, and the 60  $\mu\text{m}$  membrane presented better transparency than the 82  $\mu\text{m}$  thick membrane (Figure 4B).

### 2.4 | Mechanical Properties

The membranes obtained by cross-linking at 160°C and washing in water for 48 h were evaluated for their toughness by tensile test. The highest mechanical strength, with 1.23 MPa was recorded for 82  $\mu\text{m}$  thick membranes, proving the stability of fibrous scaffolds. All three samples of 82  $\mu\text{m}$  thick membranes demonstrated a mechanical strength of  $1.23 \pm 0.02$  MPa, maintaining the repeatability (Figure 5A). The samples of 60  $\mu\text{m}$  thickness presented a strength of 0.8 MPa on average, although the elasticity of the samples had a gap of 15% strain (Figure 5B). When the best results of each membrane were compared, 82  $\mu\text{m}$  thick membrane



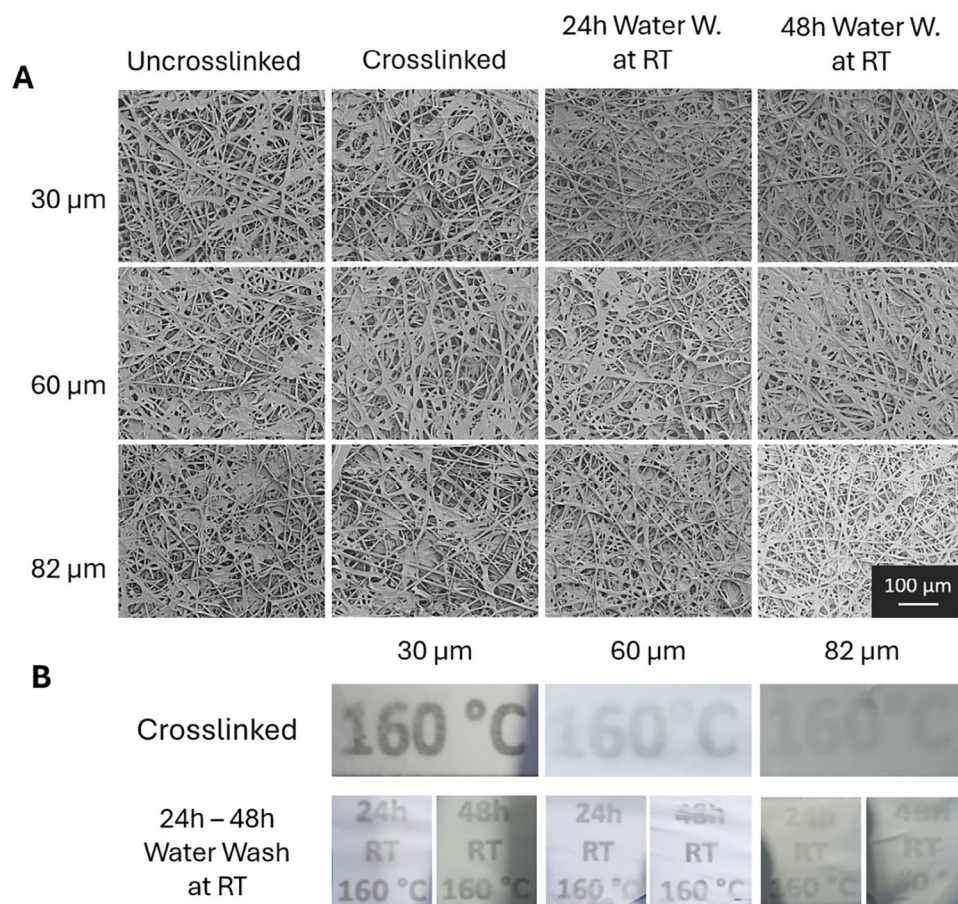


**FIGURE 4** | The comparison of membrane thickness by SEM images (A), and by transparency through the photographs taken from membranes with written text (B).

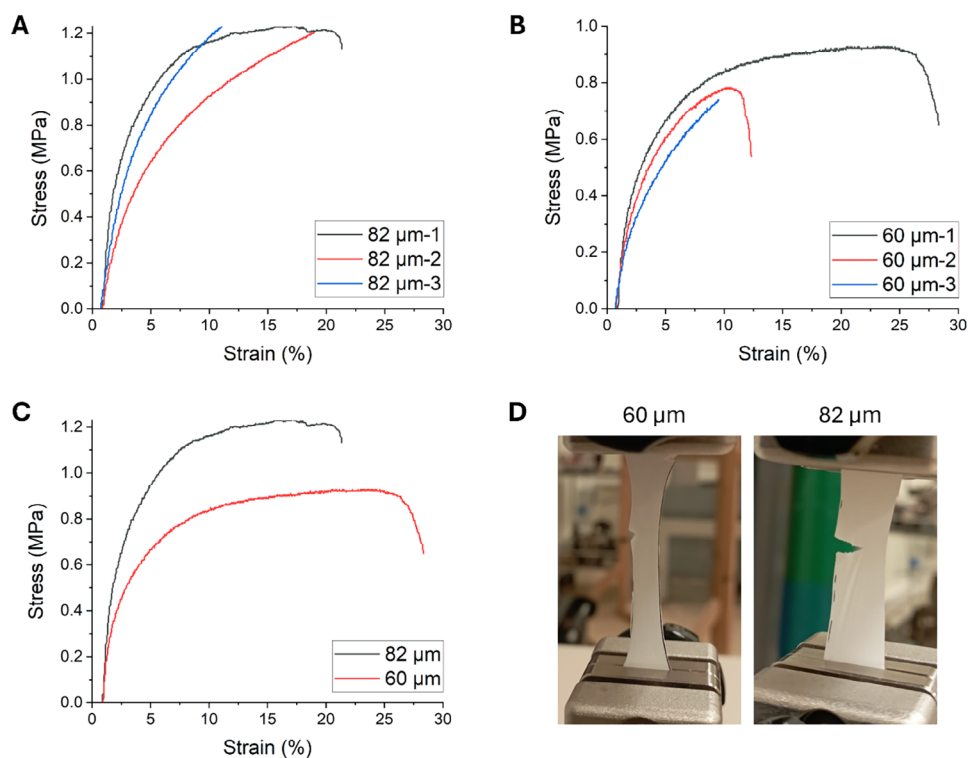


**FIGURE 5** | Mechanical strength of the membranes with 82  $\mu\text{m}$  thickness (A), 60  $\mu\text{m}$  thickness (B). Comparison of 60 (red) and 82 (black)  $\mu\text{m}$  thick membranes in stress (MPa)-strain (%) graphs (C), and images showing the break point of membranes during tensile test (D).

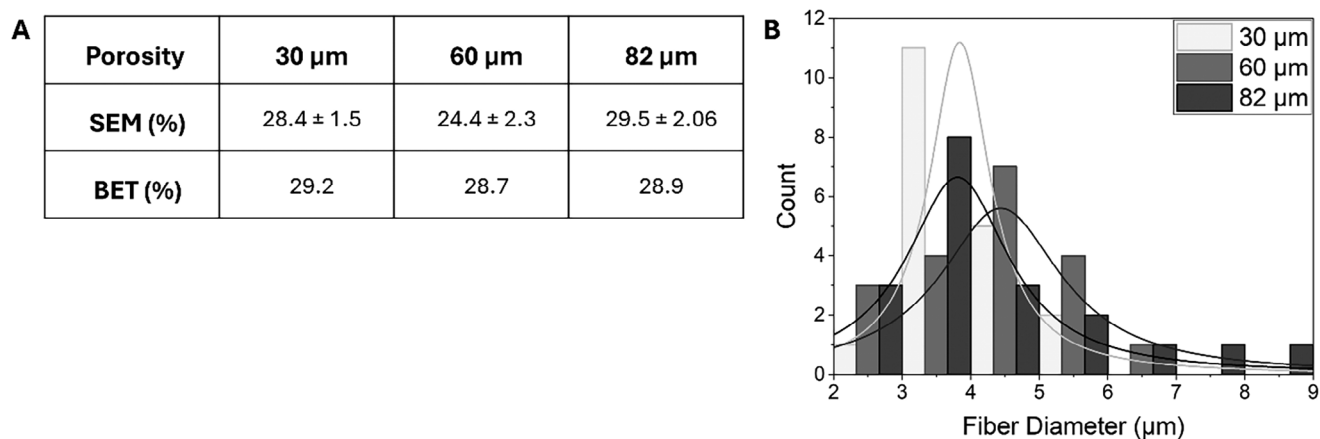


**FIGURE 6** | The percent porosity by SEM image analysis and BET gas porosity analysis (A) and the distribution of fiber diameter measurements (B) for membranes (30  $\mu\text{m}$ -light grey, 60  $\mu\text{m}$ -gray, and 82  $\mu\text{m}$ -black). For porosity calculations, three replicates were applied. For fiber diameter, 20 measurements were taken by ImageJ for 30-, 60-, and 82  $\mu\text{m}$  thick membranes and fitted in histogram analysis by Lorentz fitting.

resulted in higher strength but less elasticity than that of 60  $\mu\text{m}$  thick membrane (Figure 5C). It can also be observed from the pictures taken during the analysis (Figure 5D) that 60  $\mu\text{m}$  thick membrane has higher elasticity than 82  $\mu\text{m}$  thick membrane. The overall stress value of membranes was 1000 kPa that is significantly higher than the reported highest values of 600 and 800 kPa for PGS membranes [29, 45].

## 2.5 | Porosity and Fiber Size Measurements

The morphology of the membranes influences the cell attachment and proliferation that is necessary for in vitro and in vivo applications. The porosity of the membranes was characterized both from the SEM images and BET analysis to be precise.

The percent porosity of the 30  $\mu\text{m}$  thick membranes was calculated as 28.4%, while it slightly dropped to 24.4% for 60  $\mu\text{m}$  thick membrane and recovered to 29.5% in 82  $\mu\text{m}$  thick membrane (Figure 6A). The results of BET analysis supported the calculations on SEM images by showing 29.2%, 28.7%, and 28.7% for 30-, 60-, and 82- $\mu\text{m}$  thick membranes, respectively. Even though the thickness was increased, the percent porosity did not change significantly, proving the success of repeatability of the spinning in different volumes. The membranes facilitated an average fiber diameter of  $3.9 \pm 3 \mu\text{m}$  with no significant variation among groups (30-, 60-, and 82  $\mu\text{m}$  thickness membranes) (Figure 6B). Both 60- and 82  $\mu\text{m}$ -thick membranes maintained the initial diameter range observed in the 30  $\mu\text{m}$ -thick membranes (4.02  $\mu\text{m}$ ) but displayed a broader distribution within this range (4.27  $\mu\text{m}$  for 16 mL and 4.35  $\mu\text{m}$  for 24 mL), further confirming the consistency of the spinning process.

## 2.6 | Permeability Measurements

The continuous nutrient supply, such as glucose, is highly important for maintaining the corneal epithelial and endothelial cell integrity. It reaches to the epithelium by passing through the stroma and endothelium [46]. Therefore, it is vital to assess the rate of glucose diffusion through these membranes. The graph in

Figure S3 presents the diffusion rate of glucose through 82  $\mu\text{m}$  thick membranes. The slope of these lines provides the glucose diffusion rate value of the membrane that is used to calculate the diffusion coefficient by Equation 1. The resulting diffusion coefficient value for 82  $\mu\text{m}$  was  $9.8\text{E-}07$ , which is highly close to the natural cornea diffusion coefficient value of  $3.02\text{E-}06 \text{ cm}^2/\text{s}$  [46], therefore, indicating the success of electrospun membranes in terms of permeability.

## 2.7 | Biocompatibility Measurements

In this study, two different corneal cells were cultured on PGS membranes and their viability were evaluated by Cell Counting Kit 8 (CCK8) and Live/Dead assay. The results show that electrospun PGS-PVA membrane is biocompatible with HCEC and HCEndC culture (Figure 7). After a 1-week culture period, HCEndCs cultured on a PGS membrane had 96.5% viability compared to the control group (86.2%) (Figure 7A), suggesting the electrospun PGS-PVA membrane supports the viability of HCEndCs. On the other hand, HCECs cultured on the PGS membrane had a similar viability percentage compared to their control group (88%) after a 1-week culture period. The previous studies with PGS-PVA electrospun membranes have primarily evaluated fibroblast cell attachment reporting a 90% viability [14, 33].

The SEM images of the HCECs also support the numerical data and assay. The cells connect to each other by elongating their fibrils and attaching to the membrane (Figure 7B). The viability results were corroborated by Live/Dead assay, which indicated a population of viable HCEndCs and HCECs (Figure 7C). Based on these results, it can be stated that both cell types exhibit a high population of viable cells. However, some cells were observed to be stained by both calcein acetoxymethyl ester (Calcein AM) and propidium iodide (PI). This phenomenon may likely result from these cells experiencing stress. PI is not cell-permeable; however, under stress conditions, cell membrane permeability may change, allowing PI to enter the cells. Additionally, cells in an apoptotic or necrotic state may also exhibit permeability to both Calcein AM and PI, explaining the dual staining [47].



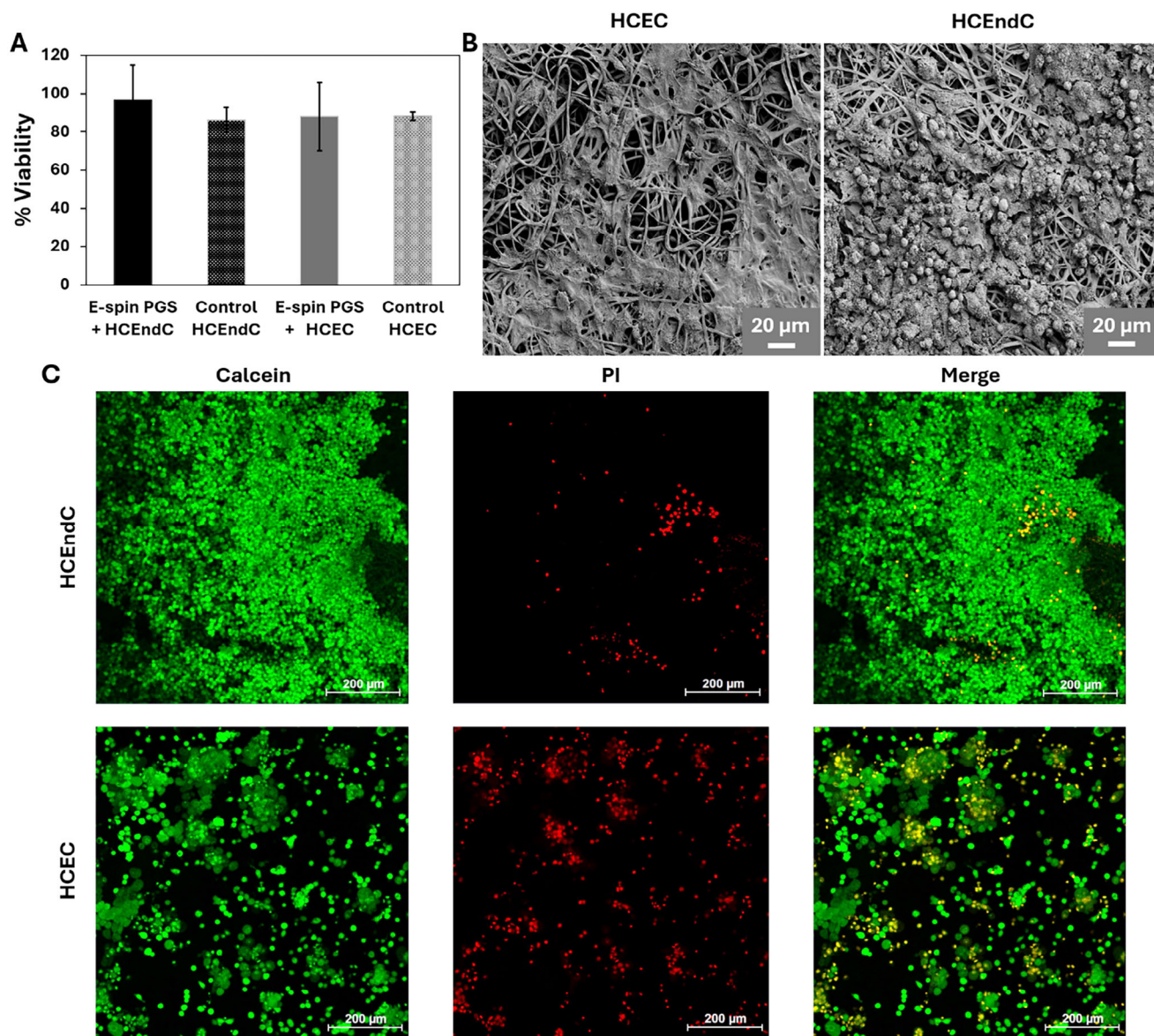


**FIGURE 7** | Biocompatibility evaluation of PGS membranes. Percent viability of corneal cells in 1 cm<sup>2</sup> area ( $n = 5$ ) where the viability of cells grew on the membranes and cells on the cell culture plate compared (A), SEM image of HCECs and HCEndCs on the PGS-PVA membranes after 1-week incubation (B), live and dead assay results indicating the Calcein and PI content in the cells and the merge of two images for HCEndCs and HCECs (C).

### 3 | Conclusions

Numerous diseases such as corneal abrasion, erosion, ulcer, and dystrophies related to corneal epithelial layer causing vision loss can be attained by tissue engineering approaches. In this regard, biomaterials that could be fabricated into transparent tissue substitutes become prominent. Therefore, in this study, we examined PGS as the transparent biomaterial and took advantage of PVA as the reinforcement to obtain electrospun membranes. We found that 160°C curing temperature and 48 h water washing are the optimal parameters to obtain fibrous and durable membranes. The membranes obtained with these parameters were highly compatible with HCECs and HCEndCs by 90% viability rate.

Here, for the first time, we report electrospun PGS membranes as potential tissue substitutes for corneal tissue engineering.

Among the promising results, it is also evident that electrospun PGS membranes exhibit lower transparency compared to the natural cornea due to high porosity and light reflection. Nonetheless, in vivo evaluation should be completed to conclude whether membranes would be degraded and regenerated over time resulting in increased transparency. Alternatively, PGS could be modified (acrylation or methacrylation) to apply alternative cross-linking strategies and also to increase viscosity allowing its electrospinning without a need for an additional polymer.



## 4 | Experimental Section

### 4.1 | Materials

PVA (Mw = 90 000, degree of hydrolysis = 98%), glycerol (purity 99%), sebacic acid (purity 99%), toluene (purity 99%), and HFIP were purchased from Merck (Germany). The sulfuric acid (H<sub>2</sub>SO<sub>4</sub>) (purity 95–98%) was purchased from ISOLAB (Germany).

Keratinocyte Serum Free Media (KSFM), KSFM supplement kit, Human Endothelial SFM, and Calcein AM were purchased from Thermo Fisher Scientific (USA). Human FGF-basic was purchased from Peprotech (London, UK). The CCK8 Cell Counting Kit 8 was purchased from GLPBIO (USA). Human corneal epithelial cells (HCECs) were obtained from Afsun Sahin's Lab (Koc Hospital, Turkey). Human corneal endothelial cells (HCEndCs) were purchased from DSMZ (Leibniz, Germany). The coating solution for HCEC culture, Collagen Coating Solution, was purchased from Cell Applications, Inc (San Diego, CA). The coating solution for HCEndC culture, FNC Coating Mix, was purchased from Athena Enzyme Systems (Baltimore, MD, USA). The Penicillin Streptomycin Solution was purchased from Pan Biotech (Germany). Propidium iodide solution was purchased from Sigma Aldrich (St. Louis, USA). Fetal Bovine Serum (FBS) was purchased from Pan Biotech, Germany.

### 4.2 | Methods

#### 4.2.1 | Synthesis of PGS Prepolymer (prePGS)

The glycerol and sebacic acid (1:0.8 molar ratio) were dissolved in toluene (8 mL) in a beaker that was covered with aluminum foil and stirred at 180°C. Once the monomers fully dissolved in toluene, H<sub>2</sub>SO<sub>4</sub> (at 1.1 × 10<sup>-3</sup> molar ratio of glycerol) was added into the solution. After 10 min mixing, small holes were made in the aluminum foil cover. The reaction was continued for an additional 34 min at 180°C under open air.

#### 4.2.2 | Fabrication of PGS Membranes

The PGS membranes were fabricated (Figure 1) by electrospinning a prePGS-PVA blend, and then, they were thermally crosslinked and finally washed for PVA removal. A prePGS and PVA (5.8 wt.% 55:45 molar ratio) blend was prepared by dissolving the polymers in HFIP overnight. Electrospinning was performed by using an 18G needle under 3.5 mL/h flow rate, 24 kV voltage, and 20 cm distance. Aluminum foil on a rotating mandrel at 500 rpm was used to collect the electrospun fibers. The fibrous membranes were placed in a pre-heated, vacuum oven at 140°C–160°C and 5 mb for 48 h. PVA was removed from the membranes with water wash up to 48 h by gently mixing.

#### 4.2.3 | Membrane Characterization

**4.2.3.1 | Chemical Cross-Linking and PVA Removal.** An FT-IR (Thermo Scientific / iS10) spectrometer with a frequency range of 400–4000 cm<sup>-1</sup> at 4 cm<sup>-1</sup> resolution was used to confirm

the chemical bonds and groups of PGS and PVA and to determine cross-linking degree.

#### 4.2.3.2 | Morphology and Fiber Size of the Membranes.

The scanning electron microscopy (SEM, Zeiss / Leo Supra VP35) was used to evaluate fiber morphology and size of the membranes by placing the samples onto conductive carbon tape on the aluminum stubs. They were coated with Au/Pd (Cressington 108 Sputter Coater) at 3.5 nm thickness (40 mA for 120 s). Fiber diameters were determined by Zeiss SEM software.

**4.2.3.3 | Porosity Measurements.** The porosity calculations were performed via ImageJ software from SEM images. Additionally, the porosity was measured by Brunauer–Emmett–Teller (BET, Micromeritics 3 Flex) analysis. The dried samples were placed in BET tubes (Micromeritics 3Flex 3500 Sample tube, Flat Bottom, 12 mm) and degassed overnight at 100°C. Then, the tubes were placed in the BET machine within liquid nitrogen to conduct the analysis with BJH Isotherm analysis parameters of N<sub>2</sub> as adsorptive in 77.203 K.

**4.2.3.4 | Permeability Measurements.** Two-sided perfusion chambers (9 mm clear Valia-Chien Cell, 2 mL, PermeGear, Inc.) were used to determine the permeability of the membranes. The membrane was washed 48 h in water at room temperature, then in ethanol for an hour. The washed and dried membrane was carefully placed in between chambers. One of the chambers was filled with only FBS where the other one was filled with glucose (10 mg/mL) in FBS. The diffusion time and the amount of glucose was recorded until the glucose amount in only FBS side reached 400–500 mg/dL. The permeability was calculated according to the Equation 1 [46] where  $D$  is the diffusion coefficient,  $L$  is the thickness of the sample,  $C$  is the first concentration of glucose measured at time zero,  $Q$  is the diffused glucose amount during time  $t$  per unit area,  $dC/dt$  is the concentration per time that is the slope of the graph of glucose diffusion and  $A$  is for the diffusion area of the chambers:

$$D = \frac{Q \times L}{C} , \text{ where } Q = \frac{dC}{dt} \quad (1)$$

**4.2.3.5 | Mechanical Properties.** A uniaxial tensile test was applied to membranes to characterize mechanical stability via Mark 10, Series 7 digital force gauge. A rectangular sample of 30 mm length and 125 mm width was prepared according to the American Society for Testing and Materials (ASTM) D882 standards for the films with a thickness less than 1 mm. A 50 N load cell was used, and the test was conducted at a rate of 10 mm/min. Each test was evaluated in triple ( $n = 3$ ).

#### 4.2.4 | Biocompatibility Assessment of Membranes

The PGS membranes were evaluated with human corneal epithelial cells for the membrane biocompatibility. PGS membranes were sterilized overnight in ethanol (70%) and exposed to UV radiation for 1 h on each side. Sterile membranes were coated with a collagen coating solution for HCECs and FNC Coating Mix for HCEndCs for 30 min at 37°C. 30 000 cells suspended in growth media were seeded on membranes placed on a hydrophobic plate. The samples were incubated for 2 h at 37°C and 5%

CO<sub>2</sub>. After incubation, samples were transferred to a 48-well cell culture plate, and the wells were filled with growth media. KSFM supplemented with EGF (0.005 µg/mL), bovine pituitary extract (BPE) (5 µg/mL), and Penicillin–Streptomycin solution (1%) was used as the growth media for HCECs. Human Endothelial SFM supplemented with FGF (10 ng/mL) and penicillin–streptomycin solution (1%) was used as the growth media for HCEndC. A 1-week culture period was carried out by changing the growth media every two days for both cell groups seeded on membranes.

At the end of the culture period, CCK8 reagent diluted with growth media (at a 1:10 ratio) was applied to samples and incubated for 4 h at 37°C. Reaction solutions were transferred to 96 well plate and measured at 450 nm with spectrophotometer (Tecan, Infinite 200 Pro). Membranes without cell seeding were used as the negative control. The same amount of HCECs/HCEndCs seeded on a 48-well plate was used as the positive controls. The maximum OD value of the positive control was accepted as 100% viable, and the viability percentages of all samples were calculated accordingly.

The samples were stained with Calcein AM and Propidium Iodide (PI) for a live and dead assay. Briefly, after washing the samples with PBS to completely remove the culture medium residues, a staining solution containing Calcein AM (1 µM) and PI (1 µg/mL) in PBS (1 mL) was prepared. The staining solution was added to the samples and incubated for 30 min at 37°C. Following incubation, the samples were washed three times with PBS for 15 min each to remove excess dye, and then observed under a confocal microscope (Zeiss L710).

To visualize the cell attachment to the membranes, the PGS samples cultured with cells for 1 week were fixed with a series of ethanol following glutaraldehyde (2.5%), and then hexamethyl-disilazane. The fixed samples were monitored under SEM with 3–5 kV.

## Acknowledgements

This work was funded by 2232 International Fellowship for Outstanding Researchers Program of TUBITAK (Grant number 118C371). Sumeyye Narin's scholarship was kindly provided by Merck GmbH. The funders had no role in study design, data collection or analysis, the decision to publish, or the preparation of this manuscript. The authors acknowledge the contributions of Kamal Asedi-pakdel in the initial stages of electrospinning optimization of the PGS.

## Conflicts of Interest

The authors declare no conflict of interest.

## Author Contributions

**Sumeyye Narin:** Writing – original draft, Investigation, Formal analysis, Methodology, Conceptualization, Visualization. **Sevilay Burcu Sahin:** Investigation, Methodology, Formal analysis. **Ebru Demir:** Investigation, Methodology, Formal analysis. **Sibel Cetinel:** Supervision, Project administration, Data curation, Funding acquisition, Conceptualization, Writing – review & editing.

## Data Availability Statement

The data that support the findings of this study are available from the corresponding author upon reasonable request.

## References

1. C. E. Ghezzi, J. Rnjak-Kovacina, and D. L. Kaplan, "Corneal Tissue Engineering: Recent Advances and Future Perspectives," *Tissue Engineering Part B: Reviews* 21, no. 3 (2015): 278–287.
2. J. W. Ruberti, A. S. Roy, and C. J. Roberts, "Corneal Biomechanics and Biomaterials," *Annual Review of Biomedical Engineering* 13, no. 1 (2011): 269–295.
3. T. Almubrad and S. Akhtar, "Structure of Corneal Layers, Collagen Fibrils, and Proteoglycans of Tree Shrew Cornea," *Molecular Vision* 17 (2011): 2283.
4. D. W. DelMonte and T. Kim, "Anatomy and Physiology of the Cornea," *Journal of Cataract & Refractive Surgery* 37, no. 3 (2011): 588–598.
5. T. J. Cutler, "Corneal Epithelial Disease," *Veterinary Clinics: Equine Practice* 20, no. 2 (2004): 319–343.
6. A. A. Torricelli, V. Singh, M. R. Santhiago, and S. E. Wilson, "The Corneal Epithelial Basement Membrane: Structure, Function, and Disease," *Investigative Ophthalmology & Visual Science* 54, no. 9 (2013): 6390–6400.
7. P. Gain, R. Jullienne, Z. He, et al., "Global Survey of Corneal Transplantation and Eye Banking," *JAMA Ophthalmology*, 134, no. 2 (2016): 167–173.
8. D. T. Tan, J. K. Dart, E. J. Holland, and S. Kinoshita, "Corneal Transplantation" *The Lancet* 379, no. 9827 (2012): 1749–1761.
9. M. Rafat, F. Li, P. Fagerholm, et al., "PEG-stabilized Carbodiimide Crosslinked Collagen–Chitosan Hydrogels for Corneal Tissue Engineering," *Biomaterials* 29, no. 29 (2008): 3960–3972.
10. P. Fagerholm, N. S. Lagali, J. A. Ong, et al., "Stable Corneal Regeneration Four Years After Implantation of a Cell-Free Recombinant Human Collagen Scaffold," *Biomaterials* 35, no. 8 (2014): 2420–2427.
11. S. Salehi, T. Bahners, J. Gutmann, S.-L. Gao, E. Mäder, and T. Fuchsluger, "Characterization of Structural, Mechanical and Nano-Mechanical Properties of Electrospun PGS/PCL Fibers," *RSC Advances* 4, no. 33 (2014): 16951–16957.
12. M. Kruse, P. Walter, B. Bauer, S. Rütten, K. Schaefer, N. Plange, T. Gries, S. Jockenhoevel, and M. Fuest, "Electro-Spun Membranes as Scaffolds for Human Corneal Endothelial Cells" *Current Eye Research*, 43, no. 1 (2018): 1–11.
13. Z. Tang, Y. Akiyama, and T. Okano, "Recent Development of Temperature-Responsive Cell Culture Surface using Poly( N - isopropylacrylamide)," *Journal of Polymer Science Part B: Polymer Physics* 52, no. 14 (2014): 917–926.
14. Y. Wang, G. A. Ameer, B. J. Sheppard, and R. Langer, "A Tough Biodegradable Elastomer," *Nature Biotechnology* 20, no. 6 (2002): 602–606.
15. J. M. Kemppainen and S. J. Hollister, "Tailoring the Mechanical Properties of 3D-Designed Poly (Glycerol Sebacate) Scaffolds for Cartilage Applications," *Journal of Biomedical Materials Research Part A: An Official Journal of The Society for Biomaterials, The Japanese Society for Biomaterials, and The Australian Society for Biomaterials and the Korean Society for Biomaterials* 94, no. 1 (2010): 9–18.
16. R. Rai, M. Tallawi, A. Grigore, and A. R. Boccaccini, "Synthesis, Properties and Biomedical Applications of Poly (glycerol sebacate)(PGS): A Review," *Progress in Polymer Science* 37, no. 8 (2012): 1051–1078.
17. I. Pomerantseva, N. Krebs, A. Hart, C. M. Neville, A. Y. Huang, and C. A. Sundback, "Degradation Behavior of Poly (glycerol sebacate)," *Journal of Biomedical Materials Research Part A: An Official Journal of The Society for Biomaterials, The Japanese Society for Biomaterials, and The Australian Society for Biomaterials and the Korean Society for Biomaterials* 91, no. 4 (2009): 1038–1047.

18. M. Frydrych, S. Román, S. MacNeil, and B. Chen, "Biomimetic Poly (glycerol sebacate)/Poly (l-lactic acid) Blend Scaffolds for Adipose Tissue Engineering," *Acta Biomaterialia* 18 (2015): 40–49.
19. Q.-Z. Chen, A. Bismarck, U. Hansen, et al., "Characterisation of a Soft Elastomer Poly (glycerol sebacate) Designed to Match the Mechanical Properties of Myocardial Tissue," *Biomaterials* 29, no. 1 (2008): 47–57.
20. Q.-Z. Chen, H. Ishii, G. A. Thouas, et al., "An Elastomeric Patch Derived From Poly (glycerol sebacate) for Delivery of Embryonic Stem Cells to the Heart," *Biomaterials* 31, no. 14 (2010): 3885–3893.
21. J. Gao, A. E. Ensley, R. M. Nerem, and Y. Wang, "Poly (Glycerol Sebacate) Supports the Proliferation and Phenotypic Protein Expression of Primary Baboon Vascular Cells," *Journal of Biomedical Materials Research Part A: An Official Journal of The Society for Biomaterials, The Japanese Society for Biomaterials, and The Australian Society for Biomaterials and the Korean Society for Biomaterials* 83, no. 4 (2007): 1070–1075.
22. F. Iorio, M. El Khatib, N. Wöltinger, et al., "Electrospun Poly( $\epsilon$ -caprolactone)/Poly(Glycerol Sebacate) Aligned Fibers Fabricated with Benign Solvents for Tendon Tissue Engineering," *Journal of Biomedical Materials Research Part A* 113, no. 1 (2025): 37794.
23. C. D. Pritchard, K. M. Arnér, R. S. Langer, and F. K. Ghosh, "Retinal Transplantation Using Surface Modified Poly (glycerol-co-sebacic acid) Membranes," *Biomaterials* 31, no. 31 (2010): 7978–7984.
24. C. D. Pritchard, K. M. Arnér, R. A. Neal, et al., "The Use of Surface Modified Poly (Glycerol-Co-Sebacic Acid) in Retinal Transplantation," *Biomaterials* 31, no. 8 (2010): 2153–2162.
25. S. Salehi, M. Fathi, S. H. Javanmard, F. Barneh, and M. Moshayedi, "Fabrication and Characterization of Biodegradable Polymeric Films as a Corneal Stroma Substitute," *Advanced Biomedical Research* 4, no. 1 (2015): 9.
26. S. Salehi, A. Grünert, T. Bohners, et al., "New Nanofibrous Scaffold for Corneal Tissue Engineering," *Klinische Monatsblätter Fur Augenheilkunde* 231, no. 6 (2014): 626–630.
27. S. Salehi, M. Czugała, P. Stafiej, et al., "Poly (Glycerol Sebacate)-Poly ( $\epsilon$ -Caprolactone) Blend Nanofibrous Scaffold as Intrinsic Bio-and Immunocompatible System for Corneal Repair," *Acta Biomaterialia* 50 (2017): 370–380.
28. P. Stafiej, F. Küng, D. Thieme, et al., "Comparative Results of Cell Culture of human Corneal Epithelial Cells (HCE) and human Corneal Keratocytes (HCK) on Electrospun Nanofiber Matrices of Polycaprolactone Blended With Poly (glycerol sebacate) and Chitosan," *Investigative Ophthalmology & Visual Science* 57, no. 12 (2016): 1263–1263.
29. E. M. Jeffries, R. A. Allen, J. Gao, M. Pesce, and Y. Wang, "Highly Elastic and Sutureable Electrospun Poly (glycerol sebacate) Fibrous Scaffolds," *Acta Biomaterialia* 18 (2015): 30–39.
30. S. Wilk and A. Benko, "Advances in Fabricating the Electrospun Biopolymer-Based Biomaterials," *Journal of Functional Biomaterials* 12, no. 2 (2021): 26.
31. A. K. Gaharwar, M. Nikkhah, S. Sant, and A. Khademhosseini, "Anisotropic Poly (glycerol sebacate)-poly ( $\epsilon$ -caprolactone) Electrospun Fibers Promote Endothelial Cell Guidance," *Biofabrication* 7, no. 1 (2014): 015001.
32. Z. Wang, M. Zhang, L. Liu, S. M. Mithieux, and A. S. Weiss, "Polyglycerol Sebacate-Based Elastomeric Materials for Arterial Regeneration," *Journal of Biomedical Materials Research Part A* 112, no. 4 (2024): 574–585.
33. M. Gultekinoglu, Ş. Öztürk, B. Chen, M. Edirisinghe, and K. Ulubayram, "Preparation of Poly (glycerol sebacate) Fibers for Tissue Engineering Applications," *European Polymer Journal* 121 (2019): 109297.
34. B. Xu, Y. Li, C. Zhu, W. D. Cook, J. Forsythe, and Q. Chen, "Fabrication, Mechanical Properties and Cytocompatibility of Elastomeric Nanofibrous Mats of Poly (glycerol sebacate)," *European Polymer Journal* 64 (2015): 79–92.
35. A. Saudi, S. Amini, N. Amirpour, et al., "Promoting Neural Cell Proliferation and Differentiation by Incorporating Lignin Into Electrospun Poly (Vinyl Alcohol) and Poly (glycerol sebacate) Fibers," *Materials Science and Engineering: C* 104 (2019): 110005.
36. D. M. Maurice, "The Structure and Transparency of the Cornea," *The Journal of Physiology* 136, no. 2 (1957): 263.
37. X. Ding, Y. Chen, C. A. Chao, Y. L. Wu, and Y. Wang, "Control the Mechanical Properties and Degradation of Poly (glycerol sebacate) by Substitution of the Hydroxyl Groups With Palmitates," *Macromolecular Bioscience* 20, no. 9 (2020): 2000101.
38. I. H. Jaafar, M. M. Ammar, S. S. Jedlicka, R. A. Pearson, and J. P. Coulter, "Spectroscopic Evaluation, Thermal, and Thermomechanical Characterization of Poly (Glycerol-Sebacate) with Variations in Curing Temperatures and Durations," *Journal of Materials Science* 45 (2010): 2525–2529.
39. C. Tsiopstias, D. Fardis, X. Ntampou, I. Tsivintzelis, and C. Panayiotou, "Thermal Behavior of Poly (vinyl alcohol) in the Form of Physically Crosslinked Film," *Polymers* 15, no. 8 (2023): 1843.
40. Q. Fan, "Fabric Chemical Testing," *Fabric Testing*, (Elsevier 2008): p. 125–147.
41. F. Flaig, C. F. Bellani, Ö. Uyumaz, G. Schlatter, and A. Hébraud, "Elaboration and Mechanical Properties of Elastomeric Fibrous Scaffolds Based on Crosslinked Poly (Glycerol Sebacate) and Cyclodextrin for Soft Tissue Engineering," *Materials Advances* 2, no. 4 (2021): 1284–1293.
42. N. Ehlers, T. Bramsen, and S. Sperling, "Applanation Tonometry and central Corneal Thickness," *Acta Ophthalmologica* 53, no. 1 (1975): 34–43.
43. J. Liu and C. J. Roberts, "Influence of Corneal Biomechanical Properties on Intraocular Pressure Measurement: Quantitative Analysis," *Journal of Cataract & Refractive Surgery* 31, no. 1 (2005): 146–155.
44. H. Shahbazi and M. Tataei, "Influence of Porosity on Transparency Behavior of  $\text{MgAl}_2\text{O}_4$  Spinel, Experiment vs Mie Theory," *Optical Materials* 90 (2019): 289–299.
45. A. G. Mitsak, A. M. Dunn, and S. J. Hollister, "Mechanical Characterization and Non-Linear Elastic Modeling of Poly (Glycerol Sebacate) for Soft Tissue Engineering," *Journal of the Mechanical Behavior of Biomedical Materials* 11 (2012): 3–15.
46. D. Myung, K. Derr, P. Huie, J. Noolandi, K. P. Ta, and C. N. Ta, "Glucose Permeability of Human, Bovine, and Porcine Corneas in Vitro," *Ophthalmic Research* 38, no. 3 (2006): 158–163.
47. S. Kari, K. Subramanian, I. A. Altomonte, A. Murugesan, O. Yli-Harja, and M. Kandhavelu, "Programmed Cell Death Detection Methods: A Systematic Review and a Categorical Comparison," *Apoptosis* 27, no. 7 (2022): 482–508.

## Supporting Information

Additional supporting information can be found online in the Supporting Information section.

**Supporting File 1:** mame70050-sup-0001-SupMat.docx.